

## OBSERVATIONS AT 610 MHz OF RADIO HALOS IN CLUSTERS OF GALAXIES

W. J. JAFFE AND LAWRENCE RUDNICK

National Radio Astronomy Observatory,<sup>1</sup> Charlottesville, Virginia

Received 1979 March 22; accepted 1979 April 30

### ABSTRACT

In a search for diffuse radio sources such as that in the Coma cluster, we made new 610 MHz observations of 32 galaxy clusters with the Green Bank 300 foot (91 m) telescope. For 20 of these clusters the interferometric observations available at the same frequency allowed us to subtract any small high-brightness sources from our data.

We detect no Coma-like halos in any other nearby clusters, although some brighter diffuse sources are visible in the interferometric maps of more distant clusters.

From the continuity of morphology of the various cluster sources we suggest that the halo sources are fossils of extended radio galaxies such as the head-tail sources.

*Subject headings:* galaxies: clusters of — galaxies: structure — radio sources: galaxies

### I. INTRODUCTION

A number of galaxy clusters, including particularly the one in Coma Berenices, contain radio sources of morphology distinctly different from that normally associated with radio galaxies or quasars (Willson 1970; Jaffe, Perola, and Valentijn 1976; Hanisch, Mathews, and Davis 1979). The Coma source is diffuse, is not directly associated with an "active" galaxy, and has a relatively steep spectrum ( $\sim 1.2$ ). Other clusters showing probably related sources include Abell 2256 (Bridle and Fomalont 1976), A2319 (Harris and Miley 1978), A2142 (Harris, Bahcall, and Strom 1977), and possibly A426 (Ryle and Windram 1968, but see discussion in § VI*b* below).

These sources are interesting because the origin of the energetic electrons radiating in them is unclear in the absence of a connection to galactic nuclei. Also, the transport of the electrons in the cluster medium at sufficient speed is difficult to explain within our current concepts of plasma physics and the nature of the medium (Jaffe 1977).

Data on these sources are scarce. Steep spectrum sources are readily found in low-frequency surveys (e.g., Viner and Erickson 1975), but the low resolution of the surveys excludes distinction between diffuse sources and steep-spectrum radio galaxies.

To broaden the observational base for discussion of these sources we undertook a survey of a group of mostly nearby clusters using a large filled-aperture telescope at an intermediate frequency, 610 MHz. This allows detection of both low-surface brightness diffuse sources and discrete sources but does not discriminate between them. However, for many of the clusters higher resolution interferometric measurements at the same or nearby frequencies are available. The latter determine the strength and structures of the smaller sources, allowing us to measure the flux, or upper limits to the flux, of any truly diffuse com-

ponent. In the other cases we can only report the total flux; this may become useful later if interferometric data becomes available.

### II. OBSERVATIONS AND CALIBRATIONS

The 300 foot (91 m) telescope<sup>2</sup> in Green Bank, West Virginia, was used as a transit instrument to make repeated drift scans through the cluster regions during the period 1977 March 25–April 2. The dish illuminated two orthogonal dipole feeds. Separate load-switched receivers on each feed were centered at a frequency of 611 MHz, and had bandwidths of 10 MHz, and system temperatures of 190 and 195 K. The two detected outputs were sampled every 6 s. This integration time yields a fluctuation of about 0.05 K in brightness temperature per polarization. Each day the drift scans through each region were offset by 11' from previous scans, up to a maximum of eight scans. Each scan was  $\geq 3^\circ$  in length, subject to the exigencies of scheduling. The cluster fields observed, and the spatial coverage obtained, are listed in Table 1.

The total system gain and beam size were determined by observations of several KPW (Kellermann, Pauliny-Toth, and Williams 1969) sources (see Table 2), whose fields were found to be relatively free of confusing sources or galactic structure, and whose straight spectra could be interpolated to 611 MHz. We found no significant declination dependence of gain or beam size from  $10^\circ < \delta < 70^\circ$ . The calibration parameters derived are also listed in Table 2.

The Westerbork Synthesis Radio Telescope (WSRT) calibration system is based on a flux density of 37.8 Jy for 3C 147 at 609 MHz. Our gain, as given in Table 2, yields an observed flux density of 37.0 Jy for 3C 147, or 2% less. We therefore use a value of  $1.06 \text{ K Jy}^{-1}$  as our gain, which improves our consistency with the WSRT scale, and is still within the errors of the

<sup>2</sup> The 300 foot telescope is operated by the National Radio Astronomy Observatory, under contract with the National Science Foundation.

<sup>1</sup> Operated by Associated Universities, Inc., under contract with the National Science Foundation.

TABLE 1  
CLUSTER REDSHIFTS AND POSITIONS, AND LIMITS TO OBSERVED FIELDS OF VIEW

Abell	$z_{cl}$	$\alpha_{cl}$	$\delta_{cl}$	$\alpha_{start}$	$\alpha_{stop}$	$\delta_{low}$	$\delta_{high}$
262.....	0.0168 <sup>a</sup>	01 <sup>h</sup> 49 <sup>m</sup> 9	+35°55'	01 <sup>h</sup> 41 <sup>m</sup> 39 <sup>s</sup>	02 <sup>h</sup> 06 <sup>m</sup> 21 <sup>s</sup>	+35°43'	+36°27'
376.....	0.0487 <sup>a</sup>	02 42.7	+36 39	02 32 48	02 48 00	+36 12	+37 06
401.....	0.075 <sup>b</sup>	02 56.2	+13 23	02 51 03	03 03 51	+12 54	+13 49
426.....	0.183 <sup>a</sup>	03 15.3	+41 20	03 06 43	03 41 13	+40 52	+41 47
478.....	0.09 <sup>c</sup>	04 10.6	+10 22	04 04 12	04 20 48	+10 05	+10 49
496.....	0.036 <sup>d</sup>	04 31.3	-13 22	04 23 30	04 46 00	-13 48	-12 53
553.....	0.067 <sup>a</sup>	06 08.8	+48 37	05 49 57	06 23 09	+47 58	+49 15
562.....	(0.131)	06 46.5	+69 20	06 24 45	06 51 45	+68 42	+69 59
568.....	0.0779 <sup>a</sup>	07 04.3	+35 08	06 56 54	67 10 06	+34 28	+35 45
576.....	0.040 <sup>a</sup>	07 17.3	+55 50	07 11 49	07 28 19	+55 11	+56 28
591.....	(0.119)	07 38.5	+44 05	07 29 52	07 47 08	+43 27	+44 44
754.....	0.0538 <sup>e</sup>	09 06.4	-09 27	08 50 26	09 25 26	-09 52	-08 46
910.....	(0.19)	09 59.1	+67 25	09 47 41	10 15 23	+66 41	+67 58
1035.....	(0.056)	10 29.2	+40 29	10 20 59	10 37 17	+38 50	+41 07
1139.....	0.0376 <sup>a</sup>	10 55.5	+01 47	10 49 38	11 02 14	+01 11	+02 28
1213.....	0.0287 <sup>a</sup>	11 13.8	+29 33	11 06 44	11 27 08	+28 53	+30 10
1367.....	0.0214 <sup>e</sup>	11 41.9	+20 07	11 29 52	11 48 04	+19 15	+20 32
1452.....	0.063 <sup>f</sup>	12 01.1	+52 01	11 51 37	12 09 07	+51 10	+52 35
1609.....	0.089 <sup>g</sup>	12 44.0	+26 43	12 36 53	12 49 11	+26 05	+27 21
1656.....	0.023 <sup>a</sup>	12 57.4	+28 15	12 49 50	13 21 02	+27 34	+28 51
1775.....	0.0695 <sup>g</sup>	13 39.6	+26 37	13 34 38	13 54 38	+26 00	+27 16
1904.....	0.0719 <sup>a</sup>	14 20.3	+48 48	14 15 05	14 34 59	+48 04	+49 21
2079.....	0.066 <sup>h,i</sup>	15 26.0	+29 03	15 18 32	15 37 44	+28 29	+29 46
2142.....	0.089 <sup>k</sup>	15 56.2	+27 22	15 38 47	16 05 17	+26 47	+28 04
2199.....	0.031 <sup>a</sup>	16 26.9	+39 38	16 07 32	16 44 56	+39 12	+40 29
2255.....	0.0769 <sup>l</sup>	17 12.2	+64 09	16 49 00	17 46 36	+63 28	+64 45
2319.....	0.053 <sup>e</sup>	19 19.2	+43 52	18 51 12	19 27 12	+43 13	+44 30
2345.....	(0.160)	21 24.4	-12 22	21 17 48	21 35 18	-12 39	+11 55
2382.....	(0.081)	21 49.3	-15 53	21 35 56	31 58 14	-16 21	-15 26
2572.....	(0.046)	23 15.9	+18 28	23 04 34	23 23 04	+17 57	+18 52
2634.....	0.0307 <sup>a</sup>	23 35.8	+26 45	23 24 05	23 42 05	+26 17	+27 12
2666.....	0.0273 <sup>a</sup>	23 48.4	+26 53	23 42 34	23 54 46	+26 56	+27 51

REFERENCES.—<sup>a</sup>Noonan 1973. <sup>b</sup>Hintzen *et al.* 1977. <sup>c</sup>Bahcall and Sargent 1977. <sup>d</sup>Corwin 1974. <sup>e</sup>Faber and Dressler 1976. <sup>f</sup>Ulrich 1978. <sup>g</sup>Ulrich 1979. <sup>h</sup>Hintzen 1979. <sup>i</sup>Colla *et al.* 1975. <sup>j</sup>Melnick and Sargent 1977. <sup>k</sup>Hintzen and Scott 1979. <sup>l</sup>Stauffer *et al.* 1979.

KPW-based calibration. We estimate the total uncertainty of our calibration, relative to the WSRT, to be 4% for point sources.

### III. BASELINE AND SMALL SOURCE REMOVAL

After calibration, data showing obvious interference were discarded. In most cases, the interference was caused by lightning, and was limited to isolated 6 s

TABLE 2  
GREEN BANK 300 FOOT TELESCOPE,  
610 MHz CALIBRATION DATA

Source 3C	$S_{610}$ (KPW interpolation) (Jy)	$T_a$ (K)	$T_a/1.08$ (Jy)
147.....	37.1	40.0	37.0
196.....	27	29.4	27.2
270.....	28	29.7	27.5
286.....	20	22.4	20.7
295.....	41.0	42.3	39.2
309.1.....	12.4	14.0	13.0
442.....	7.6	8.0	7.4

NOTE.—Gain =  $1.08 \pm 0.03$  K Jy<sup>-1</sup>; FWHP major axis =  $28'1 \pm 0'3$  at position angle  $0 \pm 3^\circ$ ; FWHP minor axis =  $23'8 \pm 0'3$ .

samples. These spurious samples were replaced by values interpolated from adjacent points. The two polarizations were then averaged to form an estimate of the total intensity.

The zero level of scans varied from day to day as a result of changes in system noise and in the Galactic background. For fields where we had no higher resolution information, the following baseline removal procedure was used. A constant value was subtracted from each scan such that  $\sim 10\%$  of the samples were negative. A crude two-dimensional contour map was then made to identify source-free regions. These regions were then used to fit a linear baseline for each scan, and the baseline was removed from the entire scan. The brightness gradients along single scans were of the order 0.5–1.0 K per degree and varied smoothly from scan to scan (i.e., over 11' in decl.) by 0.04–0.08 K per degree. This value corresponds to curvature in the background of about 0.2–0.4 K degree<sup>-2</sup>. This curvature, in turn, would result in a flux density error of the order 0.1 Jy for a point source. This rough estimate is consistent with the direct measurements (discussed below in §IV) of the level of galactic fluctuations remaining after baselining several “cleaned” fields.

In fields where WSRT observations were available, we used them to reduce confusion from background sources and from individual cluster sources. The un-

certainties which arise from this procedure are discussed below and in the comments on individual fields. All reported sources stronger than 100 mJy (sky flux density) were subtracted from our original scans using the beam response given in Table 2. The WSRT maps are complete to at least this level in a  $3^\circ \times 3^\circ$  area about their respective field centers. For further analysis, only those parts of our fields within this  $3^\circ \times 3^\circ$  area were used. A linear baseline was determined for each "cleaned" scan, excluding the  $1^\circ$  of sky centered at the nominal cluster right ascension. This baseline was then subtracted from the entire scan. We then examined a contour map of the resulting data. If a source appeared within the  $1^\circ$  square about the cluster center, we estimated its flux and angular extents using a least-squares Gaussian fitting routine.

In fields covered by the B2 surveys (Colla *et al.* 1970, 1972, 1973) we used B2 sources when no WSRT data were available. The 408 MHz flux densities were extrapolated to 610 MHz, assuming a spectral index of 0.7, or using a measured spectral index, if known. After subtraction, the procedure was the same as described for the WSRT fields. We estimate the total calibration/extrapolation error for B2 subtractions to be 9%. The total flux density of WSRT or B2 sources subtracted from each field are listed in Table 4, along with the results.

#### IV. ERRORS

The uncertainties in our estimates of flux densities and the upper limits for undetected sources are determined by background source confusion, errors in the removal of strong source confusion, and fluctuations in the nonthermal galactic emission. The error contribution from system noise fluctuations is negligible compared to these factors. The magnitude of the second error has been discussed above. The statistical behavior of the remaining (assumed isotropic) discrete source confusion is well understood, if difficult to handle analytically (Condon 1974). The properties of the galactic foreground emission are poorly understood and will only be handled in an empirical way.

The rms confusion from discrete sources can be estimated as

$$S_{\text{rms}} = \left[ \int A^2(x, y) dx dy \int_0^{S_+} dN/dS S^2 dS \right]^{1/2},$$

where  $S_+$  is the strongest source not "cleaned" from the field, and  $dN/dS = 912S^{-2.36-0.1 \ln S} \text{sr}^{-1} \text{Jy}^{-1}$  is the differential source count at 610 MHz (Willis *et al.* 1977).  $A(x, y)$  is the antenna reception pattern, which is well approximated by a two-dimensional Gaussian with the parameters given in Table 2. The predicted value of  $S_{\text{rms}}$  for the WSRT (B2) fields is calculated to be 0.07 (0.12) Jy. In Table 3 we list the measured rms fluctuations in cleaned fields containing no strong sources. The global rms fluctuations for WSRT (B2) fields are 0.10 (0.13) Jy, with a fairly small scatter for B2 fields and a range of 0.05–0.15 Jy for the WSRT fields. This is consistent with a global galactic fluctuation level of 0.06–0.07 Jy, where, because of the

TABLE 3  
RMS FLUCTUATIONS REMAINING IN CLEANED FIELDS

Abell	$b^{\text{II}}$	$l^{\text{II}}$	(Jy)
WSRT Fields			
262.....	−25	137	0.15
376.....	−21	147	0.15
401.....	−39	164	0.13
1035.....	+59	179	0.05
1904.....	+62	90	0.06
2142.....	+49	44	0.08
2319.....	+13	76	0.09
WSRT global rms.....			0.10
B2 Fields			
568.....	+18	182	0.13
1213.....	+69	202	0.16
1609.....	+89	244	0.12
1775.....	+79	32	0.15
2079.....	+56	45	0.12
B2 global rms.....			0.13

selection effects intrinsic to our sample, we have avoided areas near the galactic plane. These numbers refer to fluctuations on a scale of  $0.5$ – $1^\circ$ , since shorter scales are averaged out by our beam and larger scales are removed by our baseline procedure.

For the results listed below, then, we have estimated upper limits and errors as follows. For WSRT fields upper limits are taken as 4% of the total subtracted flux (TSF)<sup>3</sup> or  $4 \sigma_{S(W)}$ , whichever is larger. We take  $\sigma_{S(W)}$  to be 0.07 Jy for fields with low apparent galactic contribution (measured rms  $\lesssim 0.09$  Jy) or as the measured rms for fields with larger apparent galactic effect. For the two detected sources, flux density errors  $\Delta S = \max(0.04 \times \text{TSF}, \sigma_{S(W)})$  are quoted, along with position errors of  $1.1 \times (\Delta S/S) \times$  the FWHP beamwidth. For all Bologna fields we used the same procedure, with a clean limit of 9% of TSF and a  $\sigma_{S(B)}$  of 0.13 Jy. For uncleaned fields, flux density errors of 0.2 Jy (corresponding to confusion for a field "cleaned" to about a 1 Jy level) are given and upper limits equal to 4 times this value.

The Bologna beam ( $3' \times 10'$ ) is large enough so that at large redshift a significant fraction of the flux from a halo source would be picked up and included among discrete sources cleaned from the field. To account for this we have divided the upper limits of B2 fields by a correction factor. We determined this factor by calculating the ratio of peak to total flux observed with the Bologna beam for a "standard" halo source, being a circular Gaussian source with FWHP size of  $40' \times (z_{\text{coma}}/z_{\text{cl}})$ . This size corresponds to 800 kpc for  $H = 100 \text{ km s}^{-1} \text{ Mpc}^{-1}$ . This value of  $H$  will be used throughout this paper. Since the B2 survey quotes peak fluxes, this ratio represents the

<sup>3</sup> The TSF is the total flux density of those sources in a  $3^\circ$  square field surrounding the cluster which were subtracted prior to baseline removal and mapping of the field.

fraction of our standard source that would be removed by the cleaning procedure. The measured flux upper limit in each field was divided by the fraction of flux remaining to give an estimate of the upper limit on the total halo flux. The correction factor is given in Table 4*b* along with the revised upper limits. Where large, as in A1609, the correction is also uncertain, since its value depends strongly on source morphology.

#### V. SELECTION EFFECTS

Our cleaning procedure operationally defines halos to be sources bright enough to be seen with the Green Bank telescope but not so bright as to be seen at Westerbork. The first criterion requires the source antenna temperature to be  $T_a \geq 0.65$  K under average conditions; in some fields the limit was a little higher or lower. This implies a source brightness temperature of  $T_b \geq 0.65$  K  $[1 + (\theta_b/\theta)^2]$ , where  $\theta_b$  is our beam size ( $\sim 26'$ ) and  $\theta$  is the source size (FWHP). For our

“standard” halo with  $\theta = 40'(z/z_{\text{Coma}})^{-1}$ , we need  $T_b \geq 0.65$  K  $[1 + 0.42(z/z_{\text{Coma}})^2] = 0.65$  K  $(1 + 790z^2)$ . This function, plotted in Figure 1, shows that we pick up only increasingly brighter halos at larger  $z$ . The WSRT detection limit for full synthesis observations is approximately  $T_b \approx 8$  K, with some variation according to declination and observing technique; this value is plotted as a horizontal line. The limiting sensitivity of the WSRT for extended sources can be increased by subtracting out point sources and convolving the maps to a resolution equal to the size of the source being sought (matched filtering). The theoretical noise limit for this procedure is also plotted in Figure 1 for illustrative purposes, since it was not used in the data we received. The spectacular loss of sensitivity at low  $z$  is caused by the overresolution of very large sources on the shortest baseline present at Westerbork, which we have assumed to be 36 m.

We only detect sources between the Green Bank (GB) limit and the 8 K WSRT limit. These limits

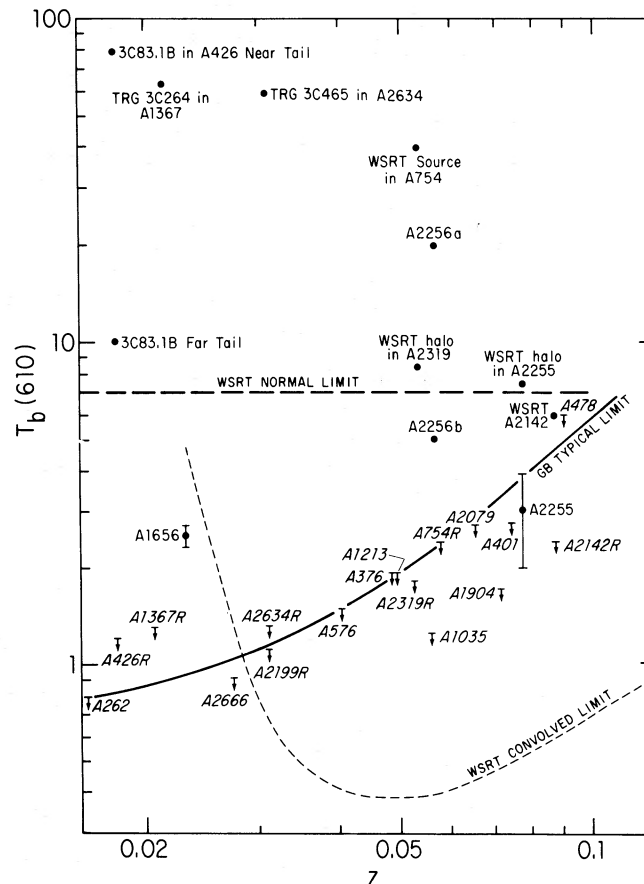


FIG. 1.—Brightness-temperature values and limits for a number of cluster radio sources. The heavy solid line shows the detection limit for our survey for a source of standard size assuming a survey flux limit of 0.6 Jy. The actual upper limits for specific clusters may lie above or below this line if the detection limits in those clusters were above or below 0.6 Jy (cf. Table 4). The symbol *R* after a cluster's Abell number indicates that the limit applies to the residual emission remaining after removal of a strong WSRT cluster source. Designations and typical brightness temperatures for these sources are given in the top part of the diagram. For further information, see § VI*b* of the text. The heavy dashed line gives the typical full-resolution WSRT detection limit. The light dashed line gives a theoretical WSRT limit after cleaning and optimal convolution. This refers only to system noise and ignores confusion and galactic foreground effects that are important at low  $z$ .



approach each other at large  $z$ , and meet near  $z = 0.08$ . Halos below the GB limit will be missed, unless they are larger than our standard source, while sources above the WSRT limit will not appear in our tabular results, but should be well characterized by the original WSRT observations. This last class of sources includes a variety of types: small radio galaxies, wide- and narrow-angle tailed sources (TRGs), larger amorphous radio sources associated with specific galaxies, and "halos" if considerably brighter than the one in Coma, which has  $T_b \sim 2.5$  K. For each of the WSRT fields we discuss the presence of such sources in § VIc below. For these fields and for the Bologna fields we include in Figure 1 the typical brightness temperatures of any such sources found, upper limits on the brightness of any additional halo components, and the measured brightnesses of our two positive detections (Coma and A2255). For the more distant clusters we used the "standard" model of the halo size in calculating brightnesses.

## VI. RESULTS

### a) Tabular Results

The results of the reduction are given in Table 4. Tables 4a, 4b, and 4c contain those fields with no clean information, B2 flux densities, and WSRT flux densities, respectively. Column (1) gives the Abell cluster designation, column (2) the redshift. Values in parentheses are  $m_{10}$  estimates. Redshift references are given in the notes to Table 1. Column (3) gives measured fluxes or upper limits, along with the correction factors mentioned above. Column (4) gives the total subtracted flux (TSF) from a  $3^\circ$  square field about the cluster center with references to the origin of the fluxes. For detected sources column (5) gives the source size parameters and (6) the offset of the source position from the cluster center. An asterisk by the cluster number indicates a note in § VI. In these notes, we indicate what relevant information is available for the noncleaned sources, as well as more detailed information on some of the cleaned fields.

### b) Discussion of Individual Fields

#### i) Noncleaned Fields

The significant measurements for 9 of the 14 non-cleaned fields reflects the fact that there is a strong association between radio sources and clusters of galaxies. As can be seen in the notes below, it is often difficult to determine the strength of possible extended emission, in the absence of a high-resolution map of the entire region.

*Abell 496.*—Owen (1974) observed several extended ( $\geq 5'$ , or blended) sources in this field, with a total flux density of  $\sim 3$  Jy at 1415 MHz. Attributing our observed flux density of  $\sim 5.2$  Jy at 610 MHz to these sources implies a spectral index of 0.65, typical for discrete extragalactic sources.

*Abell 562.*—This field was badly confused, so that our quoted flux density is only approximate. Owen *et al.* (1979) observed a total of  $\sim 2.8$  Jy in this direction at 1415 MHz, which includes the contribution from 3C 169.

*Abell 591.*—The 1415 MHz total of 0.44 Jy by Owen (1974) makes our observed flux density of 0.58 Jy appear low, if normal spectral indices are appropriate. However, the probable confusion errors make this result not significant.

*Abell 1139.*—The well-known quasar 1055+01 is projected onto this cluster, and accounts for most, if not all, of our observed flux.

*Abell 1452.*—The two strong sources in this field (Harris, Kapahi, and Ekers 1979) bracket the cluster center. The southern source has been mapped at a number of wavelengths, and shows an overall extent of  $6'$  in the single dish measurements of Owen *et al.* (1979). We could not account for the observed flux density with two unresolved sources. Because the emission seems to extend beyond the northern limits of our map, we cannot determine a total flux. In Table 4c we quote the strongest point source at the position of the southern source which would not exceed our measured brightness temperatures. This source of about 1 Jy accounts for all detectable emission towards the south of the cluster. In addition

TABLE 4a  
RESULTS FROM UNCLEANNED FIELDS

Abell (1)	$z$ (2)	$S_{610}$ (Jy) (3)	TSF (4)	Size (R.A., decl.) (5)	Offset (R.A., decl.) (6)
478.....	0.09	< 0.7	...	...	
496*.....	0.036	$4.9 \pm 0.2$	...	$(15' \pm 15', < 9')$	$(+0.5, < 1') \pm 0.6$
553.....	0.067	< 1	...	...	
562*.....	(0.131)	$3.3 \pm 0.2$	...	$(< 10, < 10)$	$(+0.1, +1)$ 0.8
576.....	0.0404	< 0.6	...	...	
591*.....	(0.119)	$0.6 \pm 0.2$	...	$(< 18, < 18)$	$(-0.1, +5)$ 5
910.....	(0.19)	< 0.6	...	...	
1139*.....	0.0376	$3.6 \pm 0.2$	...	$(< 10, < 10)$	$(+0.3, +3)$ 0.8
1452a*.....	0.063	1.0	...	0 (by definition)	$(-0.6, -4)$
1452b*.....	...	$\sim 3$	...	ext. at least $30'$	see text
2345*.....	...	$1.8 \pm 0.2$	...	$(< 12, < 12)$	$(-0.1, +2)$ 1.5
2382*.....	(0.081)	$1.0 \pm 0.2$	...	$(< 15, < 15)$	$(-0.2, < 1)$ 2.7
2572*.....	(0.046)	0.6	...	NS ridge, see text	

TABLE 4b  
BOLOGNA FIELDS

Abell (1)	$z$ (2)	$S$ (corr. fact.) (Jy) (3)	TSF (Jy) (4)
568.....	0.0779	< 0.8 (0.8)	7.1
1213.....	0.0489	< 0.6 (0.9)	4.5
1609.....	0.089	< 0.8 (0.7)	4.1
1775.....	0.0721	< 0.7 (0.8)	2.5
2079.....	0.066	< 0.6 (0.9)	3.1
2666.....	0.0273	< 0.5 (1.0)	1.0

at least 3 Jy are present in emission extending at least 30' North of the cluster.

*Abell 2345.*—Our observed flux comes primarily from the extended source seen by Owen (1974) at 1415 MHz. Its large apparent size may be partly due to confusion by the strong nearby source PKS 2124–12.

*Abell 2382.*—Most of our observed flux is probably due to the 0.7 Jy source(s), extended 7' seen by Owen *et al.* (1979). At the redshift of this cluster, the Coma cluster halo would have an 11' diameter. Our result is somewhat doubtful because of heavy lightning interference.

*Abell 2572.*—The map of this source appears to show a north–south ridge near the cluster center. A 610 MHz measurement of 1.1 Jy has been reported by Dickel *et al.* (1967), though they make no mention of this strange appearance. There is no indication of a strong galactic feature on the 820 MHz map of Berkhuijsen (1972).

#### ii) Cleaned Fields

Many of the “cleaned” clusters have been mapped at other frequencies. For a recent bibliography, see Harris (1977). Below, we note some of the features of individual clusters.

*Abell 1656 (Coma Berenices).*—This is the first halo discovered (Willson 1970) and remains the proto-

typical halo. Our 610 MHz flux has been estimated by integrating the scans, since the source is too large to be reliably estimated by Gaussian fitting. Our flux of  $2.83 \pm 0.3$  Jy is slightly lower than the  $4 \pm 1.5$  Jy reported in Jaffe, Perola, and Valentijn (1976) but still fits reasonably well on the extrapolation of the spectrum from lower frequencies, including a recent 430 MHz Arecibo measurement of  $4.5 \pm 1$  Jy (Hanisch, Matthews, and Davis 1979). It does not agree with the 610 MHz flux of  $1.2 \pm 0.5$  Jy of Valentijn (1978) measured with a 25 m dish. We believe that Valentijn overcorrected for contamination by Galactic emission. Our value of the FWHP halo size ( $35' \times 42'$ ) is slightly larger than reported by Jaffe, Perola, and Valentijn (1976), and significantly larger than the  $20' \times 20'$  of Hanisch, Matthews, and Davis (1979) at 430 MHz.

All of the WSRT sources cleaned from the cluster area were quite small in extent compared with the halo source. Most were at best only marginally resolved with the  $50'' \times 100''$  WSRT beam, and the largest was the tailed source 5C 4.81, which is  $5.5$  long, and contributes 1.2 Jy to the uncleaned map. In Coma, then, there is a clear separation in scale size between individual radio galaxies and the halo. The halo is about twice as strong as the sum of the cluster radio galaxies.

Maps before and after cleaning are shown in Figure 2. The irregularity of the lowest contours seems

TABLE 4c  
WSRT FIELDS

Abell (1)	$z$ (2)	$S$ (Jy) (3)	TSF (Jy) (4)	Size (R.A., decl.) (5)	Offset (R.A., decl.) (6)
262.....	0.0161	< 0.6	7.7 <sup>a</sup>		
376.....	0.0487	< 0.6	4.4 <sup>b</sup>		
401.....	0.075	< 0.5	5.1 <sup>c</sup>		
426*.....	0.018	< 1.4	36 <sup>d</sup>		
754*.....	0.058	< 0.6	8.1 <sup>e</sup>		
1035*.....	(0.056)	< 0.3	6 <sup>b</sup>		
1367*.....	0.0205	< 0.9	22 <sup>f</sup>		
1656*.....	0.023	$2.8 \pm 0.3$	11 <sup>g</sup>	(42', 35')	(-0 <sup>h</sup> 4, +4')
1904.....	0.072	< 0.3	6.3 <sup>b</sup>		
2142*.....	0.089	< 0.3	4.3 <sup>h</sup>		
2199*.....	0.031	< 0.6	13 <sup>i</sup>		
2255*.....	0.0769	$0.5 \pm 0.2$	5 <sup>e</sup>	(< 16, < 16)	(-0.2, +4)
2319.....	0.053	< 0.5	10 <sup>b</sup>		
2634*.....	0.031	< 0.7	18 <sup>j</sup>		

\* See text, § VI.

REFERENCES.—<sup>a</sup> Wilson *et al.* 1978. <sup>b</sup> Harris and Miley 1978. <sup>c</sup> Harris, Kapahi, and Ekers 1979. <sup>d</sup> Gisler and Miley 1979. <sup>e</sup> Harris, Costain, and Strom 1979. <sup>f</sup> Gavazzi and Perola 1979. <sup>g</sup> Jaffe *et al.* 1976. <sup>h</sup> Harris *et al.* 1977. <sup>i</sup> Gavazzi 1978b. <sup>j</sup> van Breugel 1978.

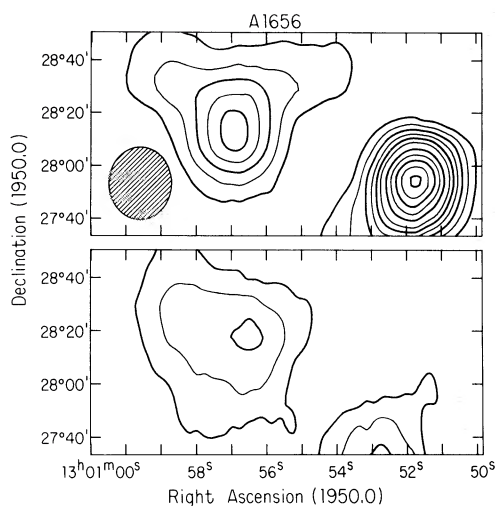


FIG. 2.—Contour maps of 610 MHz antenna temperature in region containing the Coma cluster (a) before cleaning (contours are in increments of 0.4 K up to 2 K and 0.5 K above this); the strong source at  $12^{\text{h}}52^{\text{m}}$  is 3C 277.3; ellipse at left gives FWHM beam; and (b) after removal of all point sources above 100 mJy and removal of a linear baseline. Contour increments are 0.3 K.

to be due to residual confusion from weak sources, since much of this disappears when we clean the background to sources below 50 mJy (where, however, the WSRT survey is not quite complete). We note that the source Coma A = 3C 277.3 at  $12^{\text{h}}52^{\text{m}}$  seems to be very extended to the south. There is a large residual flux (1 Jy) remaining after subtraction of a point source of 4.4 Jy at the position previously reported for this source (Jaffe, Perola, and Valentijn 1976). There are no discrete sources in any interferometric surveys of this area (Jaffe, Perola, and Valentijn 1976; Willson 1970; B2) that could explain this residual flux. 3C 277.3 is identified with a  $15^{\text{m}}5$  galaxy at  $z = 0.086$  (Schmidt 1965). If there is a low surface brightness extension of 3C 277.3, then it is at least 4 Mpc across and a member of the class of giant radio galaxies.

*Abell 426 (Perseus).*—A cluster-wide, normal spectrum ( $\alpha = 0.7$ ) halo with  $S_{408} = 12 \pm 4$  Jy was reported by Ryle and Windram (1968) using the Cambridge 1 mile (1.62 km) interferometer. We find no evidence of a halo at a limit of 1 Jy per beam (about 1 K in brightness temperature), which corresponds to a flux of about 1.6 Jy for our standard size. This agrees with a negative report by Gisler and Miley (1979). Part of the Cambridge result seems to derive from the difficulty in interpreting very short baseline interferometer measurements; the rest derives from their use of lower fluxes for the radio galaxies 3C 83.1B (NGC 1265) and 3C 84 (NGC 1275). Our higher value for 3C 83.1B comes primarily from Gisler and Miley's detection of low surface brightness extensions ( $T_b \approx 10$  K) of this tailed source filling an area of about 150 kpc square to the northeast of the galaxy. Maps before and after cleaning are shown in Figure 3.

Our limit on any additional extended emission corresponds to a brightness about 2.5 times lower than

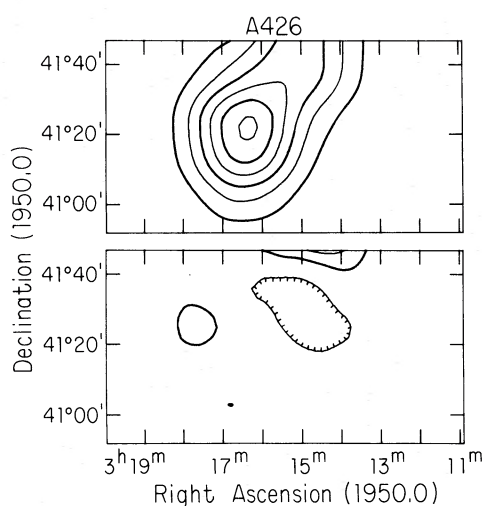


FIG. 3.—(a) 610 MHz contour map of A426. Contour levels are 4 K. (b) After removal of 3C 84, 3C 83.1B, and IC 310, contours are  $\pm 0.7$  K.

the Coma value, and a flux about 25 times less than the total strength of the separate radio galaxies there.

*A1367.*—This cluster is similar to A426 in that we find no halo above a limit of about 1 K after removal of a very extended tailed radio galaxy (TRG), 3C 264 (Gavazzi and Perola, 1979), whose extended parts have a brightness of about 60 K. Gavazzi (1978a) does find a weak ( $T_b \approx 10$  K,  $S \approx 300$  mJy), rather diffuse but somewhat clumpy source not obviously associated with any galaxy. The ratio of fluxes of radio galaxies to halo is greater than 8.

*Abell 2199.*—We detect no halo above 1.1 K after subtraction of the small strong source 3C 338 (Gavazzi 1978b).  $S_{\text{galaxies}}/S_{\text{halo}} \geq 25$ .

*Abell 2634.*—We detect no halo above about 1.3 K after removal of the wide-angle TRG 3C 465 (van Breugel 1978), whose typical brightness is about 60 K.  $S_{\text{galaxy}}/S_{\text{halo}} \geq 25$ .

*Abell 1035.*—We find no halo above 1.2 K at the cluster position, but a weak (500 mJy) source appears offset  $16'$  from the cluster center, which corresponds to 800 kpc at the cluster redshift. We do not know if this is a chance collection of weak small sources, in defiance of our confusion statistics, or a true extended source, either associated with the cluster or not.

*Abell 754.*—We detect nothing above about 2.4 K, which is about the Coma value. The cluster contains several extended sources with sizes of about 200 kpc and brightness above 60 K. These include at least one TRG and one more amorphous source (Harris, Costain, and Strom 1979; Mills *et al.* 1978).

*Abell 2319.*—We find no source. Harris and Miley (1978) report a "halo" of  $1.0 \pm 0.4$  Jy and about  $10'$ , or 400 kpc across. This has been cleaned from our measurement and we find no residual above 1.8 K. The Harris and Miley halo has about 3 times the brightness, two-thirds the diameter, and hence twice the luminosity and five times the volume emissivity of the Coma source.



*Abell 2142.*—No detection. Harris, Bahcall, and Strom (1977) report clumpy extended emission about 10' across with  $T_b \sim 6$  K not obviously associated with any optical objects. These components, which have been cleaned from our data, have also been detected at  $\lambda = 11$  cm by Haslam *et al.* (1978). Because of the large redshift, our detection limit for an additional halo is about 2.4 K.

*Abell 2255.*—Harris, Kapahi, and Ekers (1979) find several extended radio galaxies, including a TRG, embedded in a larger, fainter halo with  $T_b \approx 7$  K, diameter about 600 kpc, and a total flux of about 200 mJy. After removing the radio galaxies, but not the halo, we find a total of 500 mJy for the cluster, which corresponds to an average brightness of about 3 K for our standard model. In all likelihood this is simply an extension of the emission seen by Harris, Kapahi, and Ekers 1979*a*, but lying just below their detection limit.

#### VII. DISCUSSION

A summary of optical, radio, and X-ray data for some of the clusters observed here is given in Table 5. We include all observed clusters whose halo luminosity upper limits are less than the observed halo luminosity of Coma, or for which X-rays have been detected. Also listed is A2256, in which Bridle and Fomalont (1976) have found clumpy extended emission similar to that seen in TRGs but unconnected to any galaxy, and a smoother, more halo-like component. We have included 2695 MHz luminosities in the table because they are indicative of the radiation from small radio galaxies that dominates the spectrum at this frequency. 26 MHz luminosities are included because, in the past, a high 26 MHz flux has been interpreted as a sign of "halo" emission, on the basis of the steep spectrum seen for the Coma halo. We caution that the low-frequency measurements are by nature low-resolution measurements and in general contain no morphological information. In fact, the low-frequency flux may come primarily from relatively small, steep-spectrum components of the powerful radio galaxies present in many of the clusters observed (e.g., 3C 338 in A2199 and possibly an old TRG in A2256 [Masson and Mayer 1978]).

The chief results of this study are that smooth halos of the Coma type are relatively uncommon, and that there is no simple characteristic or combination of characteristics which can be used to predict the existence of such a halo. Figure 1 and Table 5 show six nearby clusters with detection limits substantially below the Coma brightness, and another four or five with limits near the Coma value, where no "standard" halos were found. These bracket the Coma cluster in all the variables one might think to look at to find a determinate characteristic: richness, X-ray luminosity, or presence of strong radio sources. Some unexplored characteristics, such as X-ray emission size or elliptical/spiral ratio might of course play a crucial role in determining halo luminosity.

From this we conclude that halos are probably not created by the aggregation of a large number of weak,

cluster-wide processes. If this were the case we would expect the halo luminosity to have a low variation for clusters with similar global characteristics. This conclusion disfavors halo models invoking general particle acceleration in the cluster medium, or modest particle injection or acceleration by a large number of cluster galaxies. It favors those invoking powerful events occurring infrequently relative to the lifetime of the electrons we observe at 610 MHz, about  $10^8$  years.

In only one cluster, A2255, do we find a halo source quite like that in Coma. In two others, A2142 and A2319, the WSRT data show sources that are morphologically similar, though brighter. These clusters share with Coma relatively high X-ray luminosity and the absence of any very strong radio galaxies. They each contain one or more moderate luminosity TRGs. Perhaps these conditions are necessary for smooth halo formation, but the sample is now far too small to say this conclusively.

The apparent morphological continuity between the smooth halos, the clumpier "halos" as in A2256, and the large and complex TRGs in A426, A1367, and A2634 suggests that these are all related phenomena, namely, the accumulation of past (and sometimes current) activity of strong radio galaxies. If we assume that former radio galaxies are responsible for the observed halos, then some process, as yet unclear, is required by this picture to distort and spread the emitting regions through the cluster medium until they can no longer be associated with their parent galaxies. An additional requirement is that the particle lifetime must be significantly greater in the halo than in the discrete sources, even at centimeter wavelengths. This implies that the magnetic fields in the discrete sources must be larger than the microwave background equivalent of 3 microgauss. Though this is generally observed to be true, the diffuse regions of some of the tailed sources might have lifetimes comparable to the halo. We also expect to find galaxies which are no longer active radio sources, but whose remnants are in the process of expanding into the cluster. This may be the origin of the patchy emission in clusters such as A2256.

Another class of model assumes no direct connection between the halos and extended radio galaxies, and assumes the existence of some particle-accelerating mechanism in the intergalactic medium to allow continued radiation from old electrons (Blandford and Ostriker 1978). While we cannot discount these models, they are restricted by the large variation of luminosity between similar clusters. This suggests that the acceleration process is itself highly variable in time or space.

The above discussion must remain somewhat speculative because of the small number of clusters we have observed. In addition, any statistical conclusions must await observations of a complete sample of clusters, not an ad hoc collection such as we have used. Observations like ours, using a large single dish, are relatively fast and simple; the much larger problem is acquiring a complementary set of interferometer, optical, and X-ray data.



TABLE 5  
SUMMARY OF OPTICAL, X-RAY, AND RADIO DATA FROM SOME OF THE OBSERVED CLUSTERS

Abell (1)	R (2)	RS (3)	BM (4)	$N_0$ (5)	$\Delta V$ (km s <sup>-1</sup> ) (6)	$L_x$ (10 <sup>44</sup> ergs s <sup>-1</sup> ) (7)	$T_x$ (keV) (8)	$T_e$ (610) (K) (9)	(W Hz <sup>-1</sup> ) log $L_{e10}$ (10)	(W Hz <sup>-1</sup> ) log $L_{26}$ (11)	(W Hz <sup>-1</sup> ) log $L_{2695}$ (12)
262.....	0	I	3	14	478 ± 100	0.55a	2.2-7.2	< 0.8	< -23.2	27.8	25.3
376.....	0	I	1.5	..	..	< 4.7b	2	< 1.9	< -24.2	..	..
401.....	2	cD	1	35	1390 ± 150	21.9a	5.4-8.8	< 2.7	< -24.4	29.6	27.2
426.....	2	L	2.5	33	1396 ± 140	12.4a	6.7-6.9	< 1.2	< -23.7	28.5	27.9
478.....	2	cD	3	35	..	21.4b	..	6	< -24.8	..	..
576.....	1	I	3	..	1124	< 3.6b	..	< 1.5	< -24.0	..	26.3
754.....	2	cD	1.5	30	915 ± 200	10.2b	..	< 2.4	< -24.3	..	..
1035.....	2	C	2.5	..	..	< 6.9b	..	< 1.2	< -24.0	..	..
1213.....	1	C	3	..	..	< 1.8b	..	< 1.9	< -24.2	28.9	27.5
1367.....	2	F	2.5	18	847 ± 200	0.54a	0.7-2.5	< 1.3	< -23.6	28.7	27.2
1656.....	2	B	2	28	900 ± 63	7.6a	7.9-9.9	2.4	< -24.2	28.7	26.3
1904.....	2	B <sub>b</sub>	2.5	23	..	4.5b	..	< 1.7	< -24.2	..	26.9
2079.....	1	cD	2.5	..	..	7.7b	..	< 2.7	< -24.4	..	..
2142.....	2	B	2	..	1241	34.7a	> 30	< 2.4	< -24.4	..	26.9
2199.....	2	cD <sub>p</sub>	1	19	843 ± 110	1.8a	2.2-4.9	< 1.1	< -23.8	29.4	27.1
2255.....	2	C	2.5	..	1222 ± 160	19(?)b	..	3	< -24.5	..	..
2256 <sup>a</sup> .....	2	B	2.5	32	1274 ± 255	8.9a	5-9	{(a) 20 (b) 5}	{-24.6 -23.6}	29.3	27.4
2319 <sup>b</sup> .....	1	cD	1.5	..	873 ± 140	15.7a	8.5-19.5	< 1.8	< -24.2	29.1	..
2634.....	1	cD	1.5	..	..	< 5b	..	< 1.3	< -23.8	29.3	27.7
2666.....	0	cD <sub>p</sub>	1.5	12	..	2.2a	10?	< 0.9	< -23.6	..	26.3

<sup>a</sup> Component (a) is made up of clumpy high-brightness material., similar to that seen in TRGs. Component (b) seems smoother, fainter, and covers a much larger area 500 kpc square; cf. Bridle and Fomalont 1976.  
<sup>b</sup>  $\Delta V$  quoted assumes this is one component of a double cluster. If only one cluster is assumed,  $V = 1627 \pm 220$ ; cf. Faber and Dressler (1976, 1977).

KEY TO COLUMN HEADINGS.—(1) Abell number; (2) Abell richness; (3) Rood-Sastry class from Rood and Sastry 1971 and Bahcall 1977; (4) Bautz-Morgan class, modified for easier transcription; e.g., BM class "I-II" is written as "1.5." Data are from Bautz and Morgan 1970, Sandage and Hardy 1973, Corwin 1974, and Leir and van den Bergh 1974; (5) central galaxy number (Bahcall 1977); (6) line-of-sight velocity dispersion for the cluster, from Faber and Dressler 1976, 1977; Melnick and Sargent 1977; Yahil and Vidal 1977; and Hintzen and Scott 1979; (7) X-ray luminosity; references are (a) Mushotzky *et al.* 1978 and (b) Cooke *et al.* 1978; (8) X-ray temperature from Mushotzky *et al.* 1978; (9) our measurements of and limits on halo brightness temperatures; (10) our measurements and limits on residual halo flux density assuming  $H = 100 \text{ km s}^{-1} \text{ Mpc}^{-1}$ ; (11) 26 MHz cluster luminosity from Viner and Erickson 1975; (12) 2695 MHz whole cluster luminosity from Owen 1975.

We thank the WSRT observers who supplied us with data prior to publication. These include partic-

ularly D. E. Harris, G. Gavazzi, W. van Breugel, and A. S. Wilson.

## REFERENCES

- Bahcall, N. A. 1977, *Ap. J. (Letters)*, **217**, L77.  
 Bahcall, N. A., and Sargent, W. L. W. 1977, *Ap. J. (Letters)*, **217**, L19.  
 Bautz, L. P., and Morgan, W. W. 1970, *Ap. J. (Letters)*, **162**, L149.  
 Berkhuysen, E. 1972, *Astr. Ap. Suppl.*, **5**, 263.  
 Blandford, R. P., and Ostriker, J. P. 1978, *Ap. J. (Letters)*, **221**, L29.  
 Bridle, A. H., and Fomalont, E. B. 1976, *Astr. Ap.*, **52**, 107.  
 Colla, G., et al. 1970, *Astr. Ap. Suppl.*, **1**, 281.  
 ———. 1972, *Astr. Ap. Suppl.*, **7**, 1.  
 ———. 1973, *Astr. Ap. Suppl.*, **11**, 291.  
 Colla, G., Fantì, C., Fantì, R., Gioia, I., Lari, C., Lequex, J., Lucas, R., Ulrich, M. H. 1975, *Astr. Ap. Suppl.*, **20**, 1.  
 Condon, J. J. 1974, *Ap. J.*, **188**, 279.  
 Cooke, B. A., et al. 1978, *M.N.R.A.S.*, **182**, 489.  
 Corwin, H. G. 1974, *A.J.*, **79**, 1356.  
 Dickel, J. R., Lang, K. S., McVittie, G. C., and Swenson, G. W., Jr. 1967, *A.J.*, **72**, 757.  
 Faber, S. M., and Dressler, A. 1976, *Ap. J. (Letters)*, **210**, L65.  
 ———. 1977, *A.J.*, **82**, 187.  
 Gavazzi, G. 1978a, *Astr. Ap.*, **69**, 355.  
 ———. 1978b, private communication.  
 Gavazzi, G., and Perola, G. C. 1979, in press.  
 Gisler, G., and Miley, G. K. 1979, preprint.  
 Hanisch, R. J., Matthews, T. A., and Davis, M. M. 1979, *A.J.*, submitted.  
 Harris, D. E. 1977, *Highlights Astr.*, **4**, 321.  
 Harris, D. E., Bahcall, N. A., and Strom, R. G. 1977, *Astr. Ap.*, **60**, 27.  
 Harris, D. E., Costain, C. H., Strom, R. G. 1979, in preparation.  
 Harris, D. E., Kapahi, V. K., and Ekers, R. D. 1979, *Astr. Ap. Suppl.*, submitted.  
 Harris, D. E., and Miley, G. K. 1978, *Astr. Ap. Suppl.*, **34**, 117.  
 Haslam, C. G. T., Kronberg, P. P., Waldthausen, H., Wielebinski, R., and Schallwisch, D. 1978, *Astr. Ap. Suppl.*, **31**, 99.  
 Hintzen, P. 1979, preprint.  
 Hintzen, P., and Scott, J. S. 1979, *Astr. Ap.*, **74**, 116.  
 Hintzen, P., Scott, J. S., and Tarengi, M. 1977, *Ap. J.*, **212**, 8.  
 Jaffe, W. J. 1977, *Ap. J.*, **212**, 1.  
 Jaffe, W. J., Perola, G. C., and Valentijn, E. A. 1976, *Astr. Ap.*, **49**, 179.  
 Kellermann, K. I., Pauliny-Toth, I. I. K., and Williams, P. J. S. 1969, *Ap. J.*, **157**, 1.  
 Leir, A. A., and van den Bergh, S. 1977, *Ap. J. Suppl.*, **34**, 381.  
 Masson, C. R., and Mayer, C. J. 1978, *M.N.R.A.S.*, **185**, 607.  
 Melnick, J., and Sargent, W. L. W. 1977, *Ap. J.*, **214**, 401.  
 Mills, B. Y., Hunstead, R. W., and Skellern, D. J. 1978, *M.N.R.A.S.*, **185**, 51P.  
 Mushotzky, R. F., Serlemitsos, P. J., Smith, B. W., Boldt, E. A., and Holt, S. S. 1978, *Ap. J.*, **255**, 21.  
 Noonan, T. W. 1973, *A.J.*, **78**, 26.  
 Owen, F. N. 1974, *A.J.*, **79**, 427.  
 ———. 1975, *A.J.*, **80**, 263.  
 Owen, F. N., White, R. A., Hilldrup, K., Hanish, R. J. 1979, private communication.  
 Rood, J. H., and Sastry, G. N. 1971, *Pub. A.S.P.*, **83**, 313.  
 Ryle, M., and Windram, M. D. 1968, *M.N.R.A.S.*, **138**, 1.  
 Sandage, A., and Hardy, E. 1973, *Ap. J.*, **183**, 743.  
 Schmidt, M. 1965, *Ap. J.*, **141**, 1.  
 Stauffer, J., Spinrad, H., and Sargent, W. L. W. 1979, *Ap. J.*, **228**, 379.  
 Ulrich, M. H. 1978, *Ap. J.*, **221**, 422.  
 ———. 1979, private communication.  
 Valentijn, E. A. 1978, *Astr. Ap.*, **68**, 449.  
 van Breugel, W. 1978, private communication.  
 Viner, M. R., and Erickson, W. C. 1975, *A.J.*, **80**, 931.  
 Willis, A. G., Oosterbaan, C. E., LePoole, R. S., deRuiter, H. R., Strom, R. G., Valentijn, E. A., Katgert, P., and Katgert-Merkelijn, J. K. 1977, *IAU Symposium No. 74, Radio Astronomy and Cosmology*, ed. D. L. Jauncey (Dordrecht: Reidel), p. 39.  
 Willson, M. A. G. 1970, *M.N.R.A.S.*, **151**, 1.  
 Wilson, A. S., Lari, C., Parma, P., and Vallee, J. 1978, private communication.  
 Yahil, A., and Vidal, N. V. 1977, *Ap. J.*, **214**, 347.

W. J. JAFFE: National Radio Astronomy Observatory, Edgemont Road, Charlottesville, VA 22901

LAWRENCE RUDNICK: Astronomy Department, University of Minnesota, Minneapolis, MN 55455